Effects of Moisture Content on Electrostatic Sensing Based Mass Flow Measurement of Pneumatically Conveyed Particles

Xiangchen Qian[1]*, Dengpeng Shi[1], Yong Yan[2], Wenbiao Zhang[1] and Guanguan Li[1]

[1] School of Control and Computer Engineering, North China Electric Power University, Beijing 102206, China.

[2] School of Engineering and Digital Arts, University of Kent, Canterbury, Kent CT2 7NT, United Kingdom.

* Corresponding author E-mail: xqian@ncepu.edu.cn; Tel.: 0086 01061771330

Abstract

Mass flow rate measurement of pneumatically conveyed particles is desirable for the optimal control of many industrial processes. The unpredicted variation of moisture content in particles affects the accuracy of mass flow measurement of particles in enclosed pipelines using electrostatic electrodes. In this study, the characteristics of measured electrostatic signals from particle flow under different flow conditions are analysed to study the effect of moisture content on the mass flow rate measurement. The measurement principle of ring-shaped electrostatic electrodes, the effects of moisture content on electrification of solid particles, and the experimental setup used in the study are presented. Two types of electrostatic electrodes with different axial widths and structure are adopted to measure the electrostatic signals of nonporous glass beads and porous activated carbon powder on the vertical pipeline of a 74 mm bore gas–solid two-phase flow test rig under various moisture content, mass flow rate and conveying velocity conditions. The experimental results indicate that the amplitude and frequency characteristics of the electrostatic signals change with the moisture content. The deviation of mass flow measurement that caused by the variation of moisture content is analysed, and a recalibration process is demonstrated to be effective for the improvement of measurement accuracy.

Keywords: *Gas–solid two-phase flow, moisture content, mass flow rate, electrostatic electrodes, pneumatic conveying, flow measurement*

Nomenclature

γ_{xy} Cross covariance between $x(t)$ and $y(t)$.

ε Relative permittivity of air.

ε_0 Permittivity of the vacuum.

σ_x Variances of electrostatic signal $x(t)$.

σ_y Variances of electrostatic signal $y(t)$.

τ Flow transit time.

b Coefficient for the calibration of the mass flow rate measurement of particles.

$\overrightarrow{D}$ Electric flux passing to the electrode inner surface.

$\overrightarrow{E}$ Electric field around the electrode.

f Frequency when the sphere impacts on a metal plate at regular intervals.

k_0 Constant.

k_1 Constant.

k_2 Constant.

K_c Coefficient for the calibration of the mass flow rate measurement of particles.

L Spacing between the upstream and downstream electrostatic electrodes.

n Number of impacts of an elastic sphere on a metal plate.

q_0 Initial charge on the elastic sphere.

q Electrostatic charge on an elastic sphere.

q_∞ Maximum charge on an elastic sphere.

q_s Charge on the electrode surface.

R_{xy} Cross correlation function between signals $x(t)$ and $y(t)$.

S Contact area between the elastic sphere and the metal plate.

v_c Particle velocity.

z_0 Gap between the elastic sphere and the metal plate.

1. Introduction

Pneumatic transportation of particulate material in enclosed pipelines is commonly adopted in power generation, chemical engineering, food processing, agricultural industries, etc. On-line mass flow measurement of pneumatically conveyed particles plays a vital role for the optimal control of related industrial production processes. However, the reliable measurement of mass flow rate under industrial conditions has been a challenging problem as most of the existing measurement techniques are vulnerable in industrial environment [1–3].

The electrostatic sensing technique offers a practical solution to such a measurement problem owing to its advantages of robustness, non-intrusiveness, passive measurement, cost-effectiveness and less maintenance over other techniques [4]. Law proposed an instrument, in 1975, for tracking airborne agricultural particulates based on a simple mathematical relationship between the induction current on detection electrodes and the electrostatic charges on moving particles [5]. Since then, enormous effort has been devoted to the mathematic modelling and sensing characteristics of various types of electrostatic electrodes [4,6–7], and their applications for the flow measurement of pneumatically conveyed particles under restricted laboratory conditions [4,6,8–9] and on the industrial pneumatic facilities [6,10]. In an industrial environment, particulate materials usually contain 1% to 30% moisture content, depending upon material source, storage conditions and process requirements [11]. For example, in a coal-fired power plant pulverised coal can be very wet due to open-air storage conditions. The high moisture content in particles results in weak electrostatic signals and hence unreliable mass flow measurement. When it is high enough and the temperature of conveying air is below a certain value, the electrostatic electrodes may not work as moisture vapor and coal dust can cover the surface of the sensing electrodes and form a grounded electromagnetic shield. However, little attention has been paid to the moisture content effect on the mass flow measurement using electrostatic electrodes. Emery *et al*. found that the moisture content has a strong effect on the friction property, flowability, dispersion ability and briquetting property of pneumatically conveyed particles [12]. On the other hand, high moisture content in a pneumatic conveying system may result in electric charge reduction on particles [13] and, thus, lead to errors in mass flow measurement. This phenomenon was verified by Toshiyuki *et al*., who undertook a comprehensive study of the

environment humidity effect on the tribo-charging of silicone resin coated ferrite powder. They found that the absolute value of the saturation-specific tribo-charge decreases with relative humidity and increases rapidly when the relative humidity below 30% [14]. Liang *et al*. conducted an experimental research on a 0.1 m bore pipeline with a length of 45 m under the maximum pressure of 4.0 MPa [15]. Test results showed that the mass flow rate of lignite decreases with moisture content. Moreover, the pulverised coal could not be conveyed properly when the moisture content exceeds 8.18% by weight under dense-phase flow conditions [15].

This study investigates the effects of moisture content on the electrostatic sensing based mass flow measurement of gas–solid two–phase flow. Two types of ring–shaped electrodes, which are exposed and insulated to the particle flow, are adopted in this study to measure the electrostatic signals for the derivation of the solids mass flow rate. Experimental tests were conducted on a 74 mm bore particle flow test rig using two kinds of materials, namely glass beads and activated carbon powder, with different chemical compositions and physical structures under various moisture content, mass flow rate and particle velocity conditions. The effects of moisture content on the mass flow measurement are analysed based on the characteristics of measured electrostatic signals.

2. Principle of mass flow measurement and effects of moisture content on electrostatic sensing

Electrostatic sensing based mass flow measurement is realised by measuring the velocity and volumetric concentration of pneumatically conveyed particles. In the present study, the particle velocity is measured using the cross-correlation velocimetry, which essentially measures the similarity between two signals and, thus, enjoys a high degree of immunity from the properties of particles and external conditions [6]. The measurement of particles volumetric concentration is based on the induced charge level on an electrostatic electrode. However, the charge level is influenced greatly by moisture content as it not only affects the relative permittivity of conveying air [16–17], but also the electrification property of the particles [18] during the transportation. The following sections present the principles of mass flow rate measurement and moisture content effect on the electrification of pneumatically conveyed particles.

2.1. Principle of mass flow measurement

The movement of particles in a pneumatic pipeline generates a certain amount of electrostatic charge on its surface due to particle-air frictions, particle-wall collisions and particle-particle interactions [19]. The amount of charge carried on particles can be detected by a metallic electrostatic electrode in conjunction with an electronic circuit [10,20–21]. The mass flow rate of the particles is determined from

$$q_{m,s} = K_c v_c{}^b A_{rms} \tag{1}$$

where v_c is the particle velocity (m/s), A_{rms} is the root-mean-square value of measured electrostatic signals (or rms charge level) and K_c is a constant which is flow conditions and particle velocity dependent [2,22]. In earlier studies [10,22], K_c and b are determined through experimentations over a wide range of mass flow rates and velocities of particles. As the particle velocity also affects the rms charge level [23], the measurement of the particle velocity is vital for the mass flow measurement. The mean particle velocity is determined using the following equation [6,10,21]:

$$v_c = \frac{L}{\tau} \tag{2}$$

where L is the axial distance of two identical parallel electrodes and τ is the transit time taken by the particles moving from the upstream electrode to the downstream electrode [6]. The measured particle velocity can fluctuate significantly and become unreliable if the spacing is too large as the correlation coefficient can be very low in such cases, while a very short spacing may cause interference between the sensing fields of the electrodes. Although the particle velocity is different from the conveying air phase, the slip velocity between the two phases is stable and small when the flow conditions remain steady [22]. The transit time τ is determined from the location of the dominant peak in the correlation function [6,10]. The cross-correlation function between the two signals $x(t)$ and $y(t)$ is defined as follows:

$$R_{xy}(t) = \frac{\gamma_{xy}(t)}{\sigma_x \sigma_y} \tag{3}$$

where γ_{xy} is the cross covariance between $x(t)$ and $y(t)$, and σ_x and σ_y are the variances of the two signals, respectively.

2.2. Effects of moisture content on electrostatic sensing

Matsusaka *et al.* [18] studied the charge transfer during the impact of an elastic sphere on a metal plate. The electrostatic charge carried on the sphere by repeated impacts is

$$q = q_0 \exp(-\frac{n}{n_0}) + q_\infty[1 - \exp(-\frac{n}{n_0})] \tag{4}$$

where

$$n_0 = (\frac{k_0 k_1 \varepsilon \varepsilon_0 S}{z_0} + \frac{k_2}{f})^{-1} \tag{5}$$

$$q_\infty = \frac{V_c}{k_0 + (k_2 \, z_0 / k_1 \varepsilon \varepsilon_0 S f)} \tag{6}$$

n is the number of impacts, q_0 is the initial charge on the sphere, ε_0 is the permittivity of the vacuum, ε is the relative permittivity of air, S is the contact area, z_0 is the gap between the contact bodies, f is the frequency when the sphere impacts at regular intervals, and k_0, k_1, and k_2 are constants. Since the electrostatic charge on the sphere by means of impact is related to the relative permittivity of air, which depends on moisture content according to Equation (4), the increased moisture content has a negative impact on electrostatic charging as the relatively humidity of the air phase increases with moisture content in the solids phase due to water evaporation.

On the other hand, according to Gauss's law, the induced charge on the outer surface of the electrode is equal to the flux passing to its inner surface [16–17].

$$q_s = \int_s \vec{D} ds \tag{7}$$

where

$$\vec{D} = \varepsilon \varepsilon_0 \vec{E} \tag{8}$$

q_s is the charge on the electrode surface, $\vec{D}$ is the electric flux and $\vec{E}$ is the electric field. Equation (8) implies that the electric flux reduces with the moisture content when particles transpiring in the conveying process, thus, resulting in weaker induced charge on the electrode.

3. Experimental set-up

3.1. Electrostatic electrode

Both exposed and insulated ring-shaped electrodes are used in this study to compare their performance on mass flow measurement for different moisture contents. The cross-sectional views of the exposed

and insulated electrostatic electrodes are shown in Figure 1.

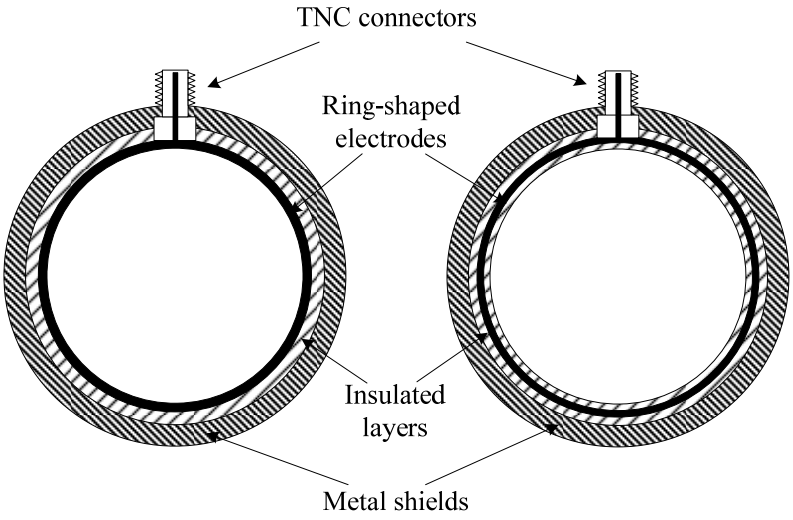

(a) Exposed electrode (b) Insulated electrode

Figure 1. Cross-sectional views of electrostatic electrodes.

As can be seen from Figure 1, the difference between the exposed and the insulated electrostatic electrodes is that the later one has an insulation polyoxymethylene (POM) layer between the inner surface of the electrode and the particle flow. In consideration of the effect of axial width on the sensing characteristics of an electrostatic electrode, two sets of electrostatic electrodes with axial widths of 2 mm and 10 mm are housed in a stainless steel sensing head and insulated from each other using POM. The electrodes are made from a piece of copper plate with 0.5 mm thickness.

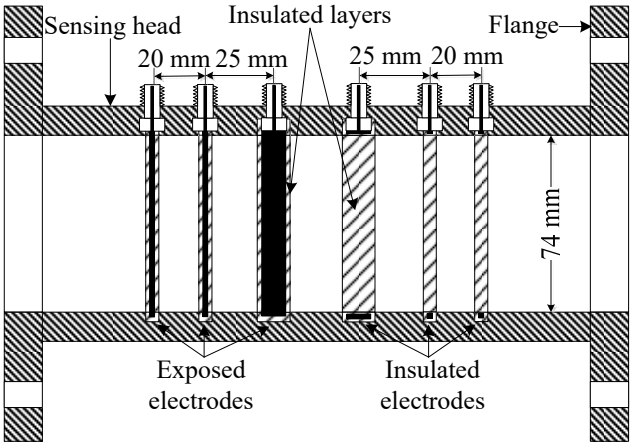

(a) Cross-sectional view

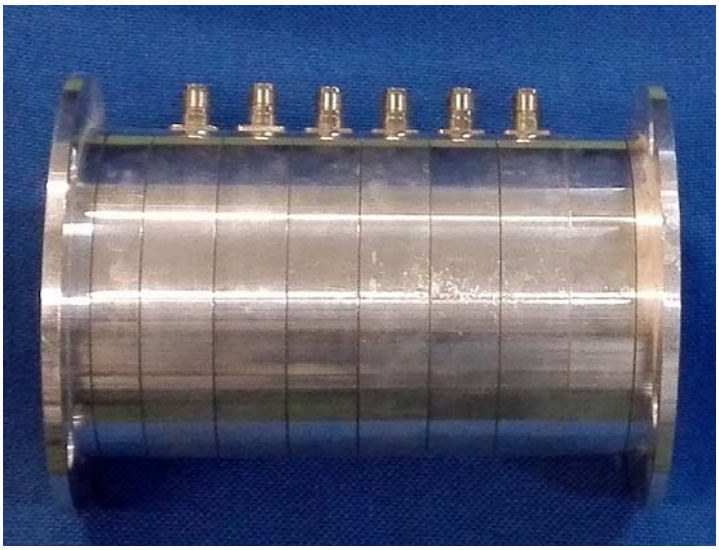

(b) Photo of the sensing head

Figure 2. Structure of the electrostatic sensing head.

Figure 2 shows the longitudinal view of the sensing head. As can be seen from Figure 2(a), the inner surface of the sensing head is made flush with the inner pipe wall. Two pairs of identical electrodes with an axial width of 2 mm are used to determine the velocity of particles through cross-correlation velocimetry as they have a wider sensing bandwidth and higher sensitivity to time-varying signals [4]. Meanwhile the two 10 mm width electrodes are applied to measure the rms charge level of particles due to their larger sensing volume and better spatial filtering effect [2,6–7]. In this study the spacing between the two adjacent narrow electrodes and that between the wide and narrow electrodes were set at 20 mm and 25 mm, respectively, based on previous studies [6,10,21,22]. Figure 2 (b) shows a photo of the electrostatic sensing head. A grounded metal layer is inserted between two adjacent electrodes to avoid their mutual interference. Six channels of electrostatic signals from the exposed and insulated electrodes are separately transmitted to two identical signal conditioning and processing circuits, as illustrated in Figure 3, using independent screened cables with Threaded Neill–Concelman (TNC) connectors on the sensing head. The electronic circuit essentially converts the weak electrostatic current signals into voltage signals with proper magnitude and filters the unwanted high frequency and power frequency noises. A NI USB-6363 data acquisition card with a sampling frequency of 25 kHz and 12 bits resolution is used to collect the raw signals. The digital signals are then fed to a digital signal processor (DSP) for the computation of flow parameters.

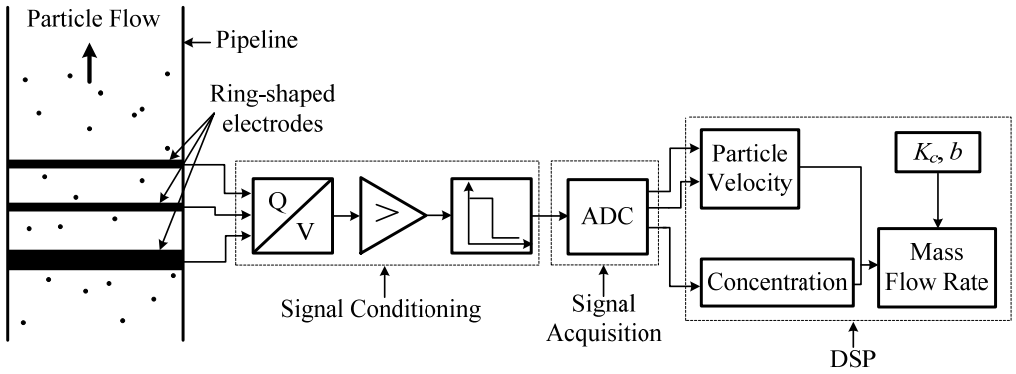

Figure 3. Signal conditioning and processing procedure.

3.2. Test rig

Experimental tests were conducted on a 74 mm bore gas–solid two-phase flow rig, as shown in Figure 4. This negative-pressure pneumatic conveyor system mainly comprises several detachable stainless steel pipe sections, a vacuum system with a receiving hopper and a precision screw feeder. Both the suction power of the vacuum system and the feeding rate of the screw are continuously adjustable to keep the air velocity and the mass flow rate of particles at required values in the repeated tests. The screw feeder provides a fixed and stable mass flow rate of particles with the aid of an embedded electronic control system. Furthermore, an off-line calibration process was conducted using a weighing device to ensure the performance of the feeder. A receiving hopper is connected to the vacuum system to recycle solid particles. As can be seen from Figure 4, the electrostatic sensing head was installed on the upper vertical section of the rig to avoid the flow turbulence caused by the elbow. The velocity of conveying air is obtained using a differential pressure anemometer (KIMO MP210) through repeated measurements on the diameter of the pipe cross-section. The anemometer has an accuracy of ±0.5% within a measurement range from 5.1 m/s to 100 m/s.

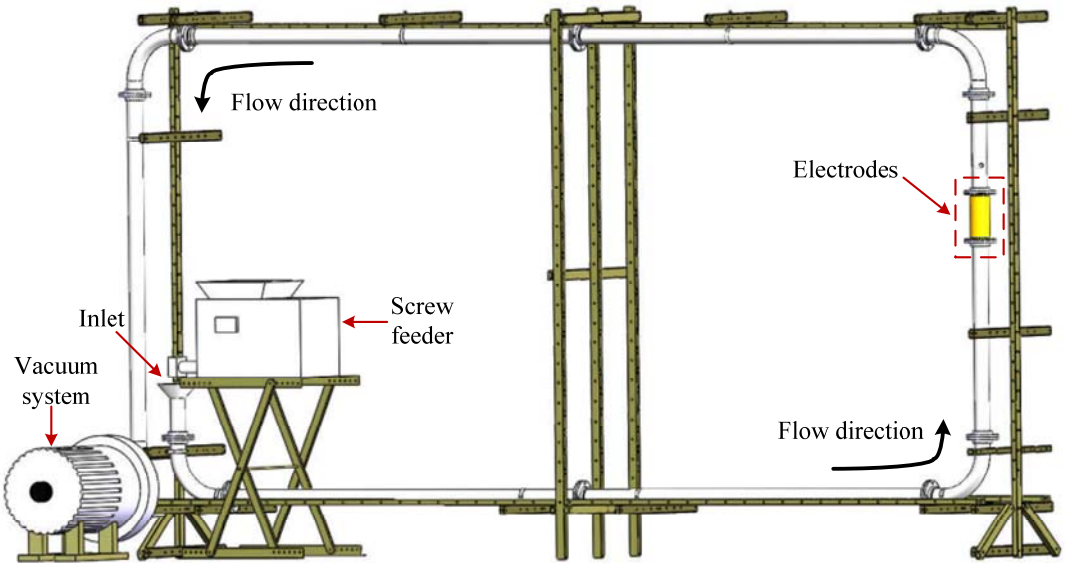

Figure 4. Layout of the 74 mm bore gas–solid flow test rig.

4. Experimental results

4.1. Test program and material properties

Table 1. Properties of typical materials

Material	Chemical composition	Appearance	Density (g/cm^3)		Diameter range (μm)	Physical structure
			Bulk	True		
Glass beads	SiO_2	milky white powder	1.5–1.8	2.2–2.7	150–200	nonporous
Silicon carbide	SiC	black powder	1.2–1.6	3.2–3.3	50–100	nonporous
Activated carbon	C	dark black powder	0.3–0.5	2.0–2.2	50–100	porous
Pulverised coal	C	black powder	0.4–0.5	1.2–1.8	60–90	porous

A series of experimental tests was conducted using two types of representative material, glass beads and activated carbon powder. The ambient temperature and relative humidity in the laboratory during the tests were 23.8˚C and 40%, respectively. Glass beads represent nonporous materials, which are widely used in sand blasting, coating and mineral powder production. For example, silicon carbide, a nonporous material, is used as wear-resistant coating in order to achieve the properties of high temperature and wear resistance in a pneumatic conveying system. Activated carbon powder is similar to pulverised coal, the most common fossil fuel used at thermal power plants, in terms of porous

structure and chemical composition. A comparison of the key properties between the two kinds of materials is shown in Table 1. As can be seen from Table 1, glass beads and activated carbon powder have similar properties in comparison with silicon carbide and pulverised coal, respectively. Glass beads are made up of silicon oxide with nonporous physical structure whereas activated carbon is a form of carbon processed to have small, low-volume pores which creates higher ability of water absorption compared to glass beads while their true densities are very close.

Table 2 lists the glass beads test conditions (TCs) under three different moisture contents and mass flow rates when the particles velocity was measured at 12.5, 17.5, 20.0 and 21.5 m/s (namely v_1, v_2, v_3 and v_4), respectively. The moisture content is defined as the mass ratio of moisture to the particles per unit volume in this study. Three different moisture content conditions, 2.1%, 5.6% and 7.8% were created during the tests by adding a certain amount of water to the glass beads. The total length between the feeding and measurement point was about 5.5 m. The moisture content in the particles reduces in the sensor point due to pneumatic drying, however, the evaporated water is still in the flow (mixed with conveying air). A “preheat” process for about two minutes was also performed to allow the characteristics of the flow reach a relatively steady state. Meanwhile, three mass flow rates of particles, i.e. 2.74 g/s, 4.12 g/s and 5.48 g/s, which are equivalent to the volumetric concentration of about 0.002%, 0.003% and 0.004% at an air velocity of 12.5 m/s, were set to study the levels of measurement errors under variable dilute glass beads flow conditions. It should be pointed out that the pipeline diameter used in this study is smaller than most of those in industry. However, the volumetric concentration of solids created on the test rig is comparable to that in industry such as coal fired power stations [24].

Table 2. Test matrix of glass beads

Mass flow rate (g/s)	**Moisture content (%)**		
	2.1	**5.6**	**7.8**
2.74	TC1	TC2	TC3
4.12	TC4	TC5	TC6
5.48	TC7	TC8	TC9

Because of the difference in moisture absorption and physical structure, moisture contained activated

carbon powder shows worse flowability as the moisture molecules are adhered to the surface and absorbed inside the particles to form moisture bonds, thereby causing the particles to cohere [25]. On the other hand, particles with a finer size range are less free flowing for there is a natural force of attraction between particles that increases with decreasing size [25]. Therefore, the test matrixes for both materials were not the same in the present study. The TCs of activated carbon tests are summarised in Table 3. Different moisture content and mass flow rate conditions were adopted in the experiments. The mass flow rate of 5.14 g/s is equivalent to a volumetric concentration of about 0.01% when the air velocity is 12.5 m/s.

Table 3. Test matrix of activated carbon

Mass flow rate (g/s)	**Moisture content (%)**	
	3.5	**6.7**
5.14	TC10	TC11

4.2. Glass beads results

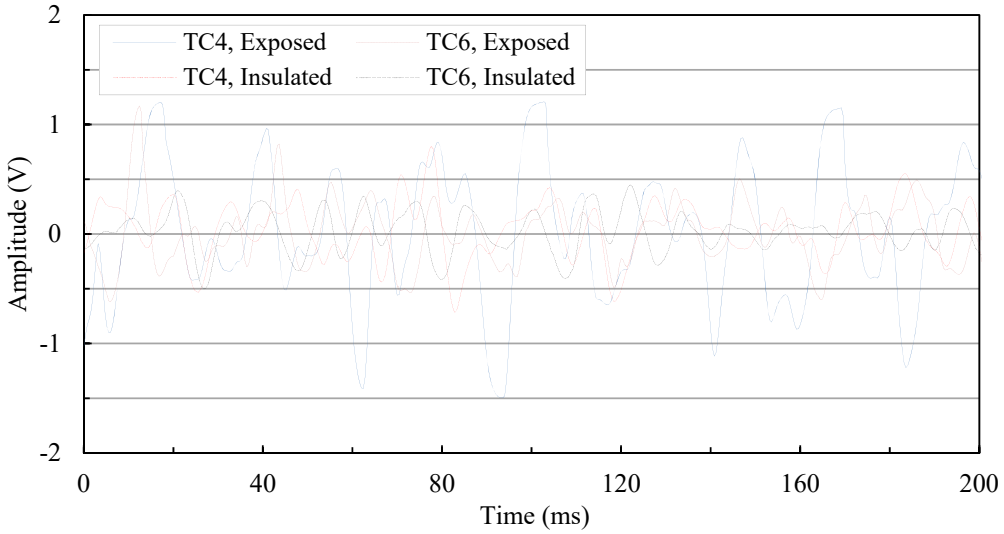

Figure 5. Electrostatic signals of glass beads under different moisture content conditions.

Figure 5 shows the raw electrostatic signals measured by both exposed and insulated electrodes with 10 mm axial width under TC4 and TC6, respectively, when the particle velocity was v_2. As can be seen from Figure 5, the fluctuation range of electrostatic signals becomes smaller with the increase of moisture content. The maximum absolute value of electrostatic amplitude is over 1.43 V under TC4, while the value is less than 1.15 V under TC6. The mean absolute rms values from the exposed and

insulated electrodes under the two conditions are 0.45 V, 0.24 V and 0.20 V, 0.15 V, respectively. Furthermore, the electrostatic signals from the exposed electrode fluctuate more significantly than those from the insulated ones. That is partly because certain particles contact the inner surface of the exposed electrodes randomly.

The moisture content affects not only the magnitude of the measured signals but also the frequency characteristics of the signals. Therefore, the signal power spectral density (PSD) can indicate the variation in moisture content in particles. Figure 6 shows the PSD of electrostatic signals under TC4, TC5 and TC6. The dominant frequencies from the exposed electrode under TC4, TC5 and TC6 are 513 Hz, 464 Hz and 439 Hz, respectively, while 562 Hz, 537 Hz and 512 Hz are determined from the signals of the insulated electrode. It is noticeable that the dominant frequency of electrostatic signals trend to decrease with the moisture content and those of the insulated electrode are higher under the same test condition. In other words, a smaller main frequency entails higher moisture content of particles which can be used as a reference for recalibration in mass flow measurement.

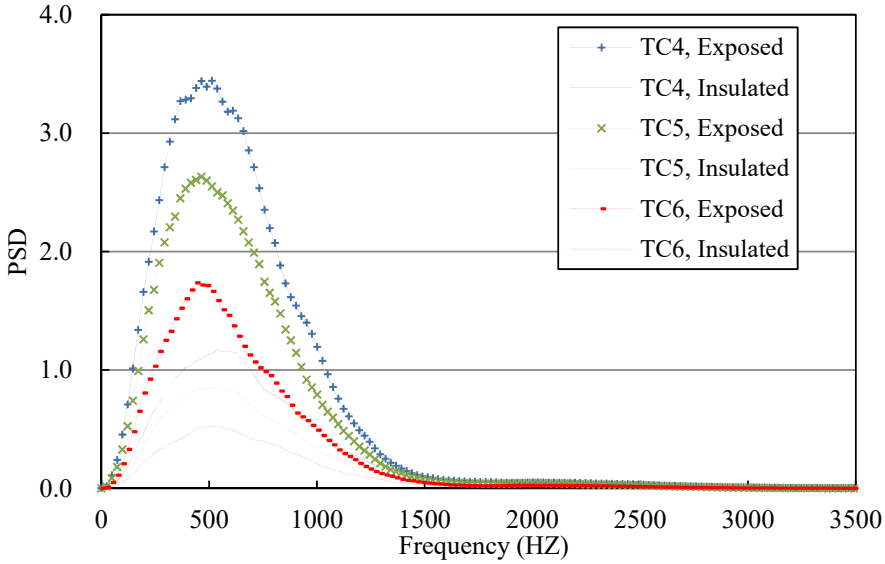

Figure 6. PSD of the electrostatic signals for glass beads under different moisture content conditions.

Figure 7 shows the measured rms values using the 10 mm insulated electrode under TC1 to TC 9 when particle velocities are v_1 and v_3. It is evident that electrostatic charges reduce with the moisture content. Furthermore, the reduction of rms value is greater under higher particle velocity condition. For example, the rms value reduces 1.02% with every percentage increase in moisture content when

moisture content increases from 2.1% to 7.8% (particle velocity is v_3 and mass flow rate is 5.48 g/s), while the reduction of rms value is only 0.64% when particle velocity is v_1.

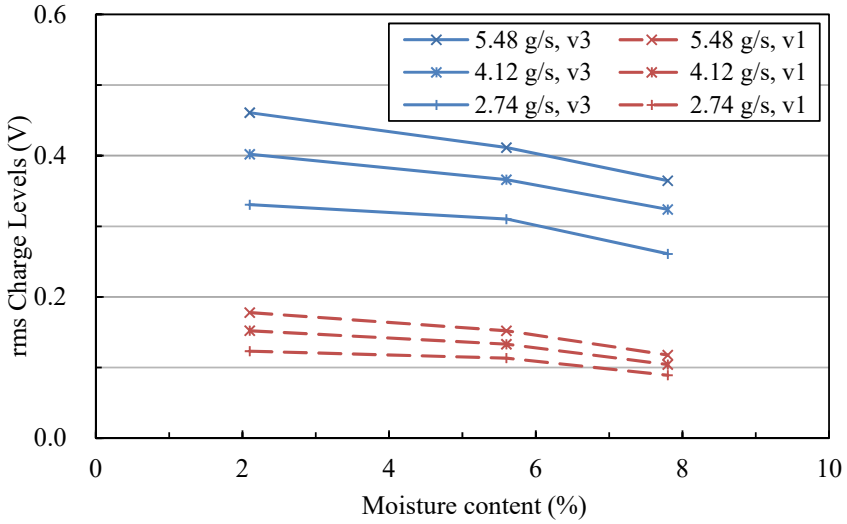

Figure 7. rms charge levels of glass beads under three different moisture content conditions.

The evaluation of the effect of moisture content on mass flow rate measurement starts with relatively simple conditions when the mass flow rate and velocity of glass beads are fixed and the moisture content is the only variable. Figure 8 shows the measured rms charge levels and the mass flow rate of glass beads (derived using Equation (1)) using 10 mm width insulated electrode under TC1, TC2 and TC3 when particle velocity is v_2. The CFTool embedded in MATLAB was used to determine K_c and b based on the least-square method.

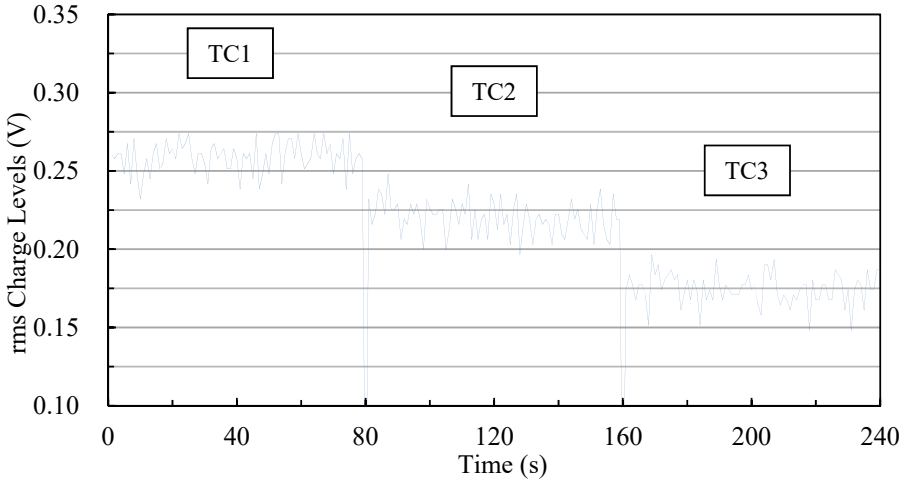

(a) rms charge levels.

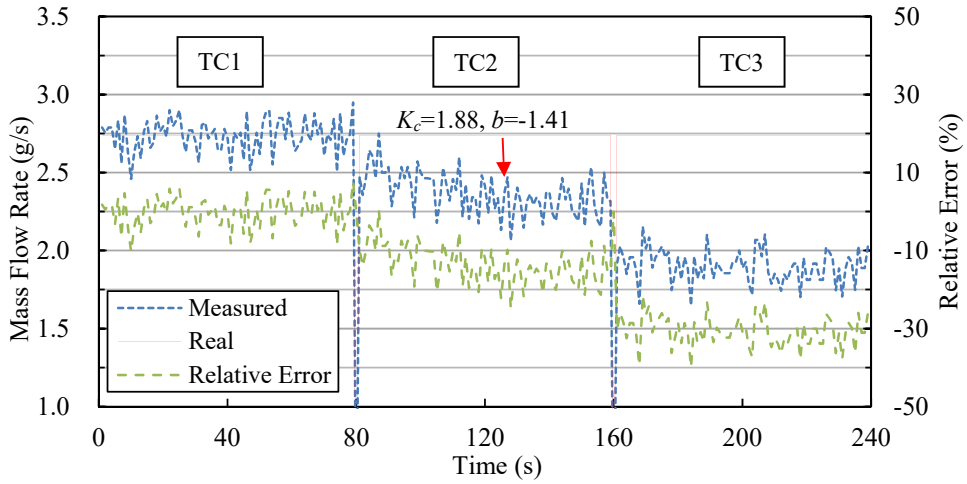

(b) Measured mass flow rate under different moisture content conditions.

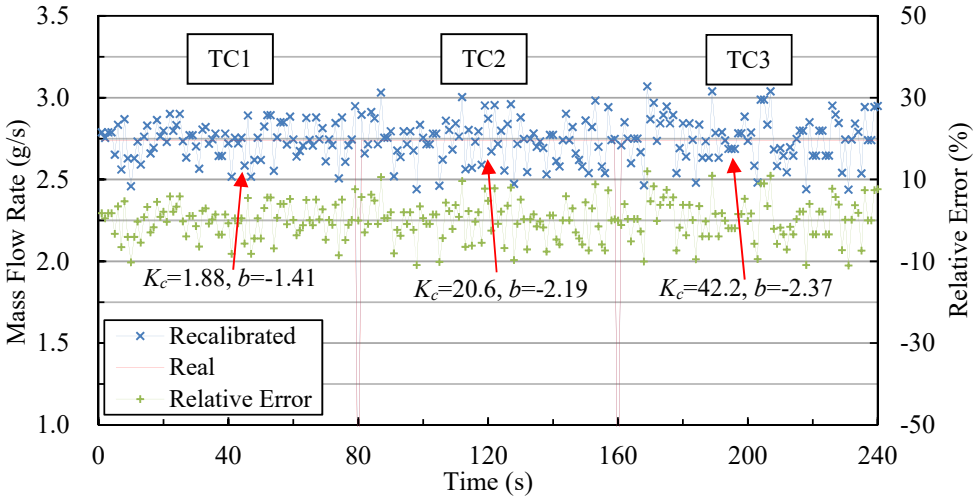

(c) Recalibrated mass flow rate under different moisture content conditions.

Figure 8. Measured and recalibrated results under TC1, TC2 and TC3.

The coefficients K_c and b that are determined using the test data under TC1 are applied to TC2 and TC3. It can be seen from Figure 8 that moisture content influences the accuracy of the mass flow rate measurement, and the relative errors become greater with the moisture content. The relative error varies within the range of ±11% when the glass beads have a moisture content of 2.1%. However, the error increases up to a maximum of ±39%, which is unacceptable in application, when the moisture content increases to 7.8%. Therefore, experimental data under TC2 and TC3 are used independently to determine K_c and b for each test condition, and the recalibrated results are shown in Figure 8 (c). Although the relative errors under TC2 and TC3 are still slightly greater than those under TC1, the relative errors of the measured mass flow rate under three moisture conditions are reduced to ±13%

with standard deviations 0.11, 0.13 and 0.16, respectively.

Further experimental tests were conducted under TC1, TC3, TC7, TC9 and all four particle velocity conditions. As shown in Figure 9 (a), the rms charge level is proportional to the velocity and mass flow rate of particles. The measurement and recalibrated results under TC1 and TC3 are shown in Figure 9 (b) and those under TC7 and TC9 are shown in Figure 9 (c). As shown in Figure 9 (b) and Figure 9 (c), the measured values under TC3 and TC9 using the same coefficients K_c and b as TC1 and TC7, respectively, have greater error because of the higher moisture content. To solve this problem, coefficients K_c and b are recalibrated using the test data obtained under TC3 and TC9, respectively, instead of those under TC1 and TC7. As a result, the recalibrated error is improved and remains under ±20% in all four velocity conditions. The standard deviations of recalibrated values in Figure 9 (b) and Figure 9 (c) are 0.19 and 0.30, respectively. However, the error is greater than that shows in Figure 8, in which the moisture content is the only factor. It is suggested that the combined effect of particle velocity and moisture content is larger than that of the individual. Therefore, it is ideal to calibrate the electrostatic system under different moisture conditions for more reliable mass flow rate measurement.

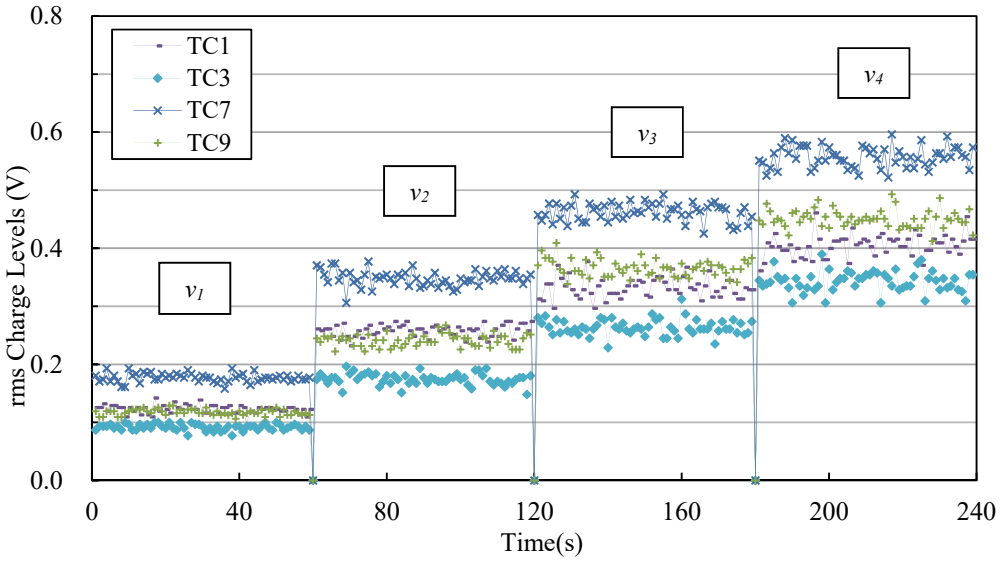

(a) rms charge levels.

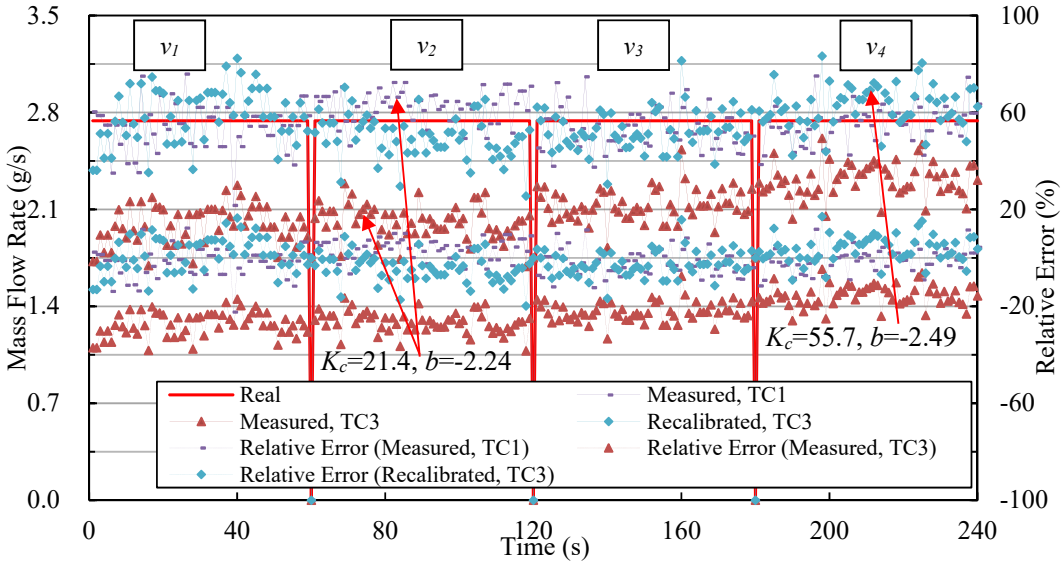

(b) Measured and recalibrated results under TC1 and TC3.

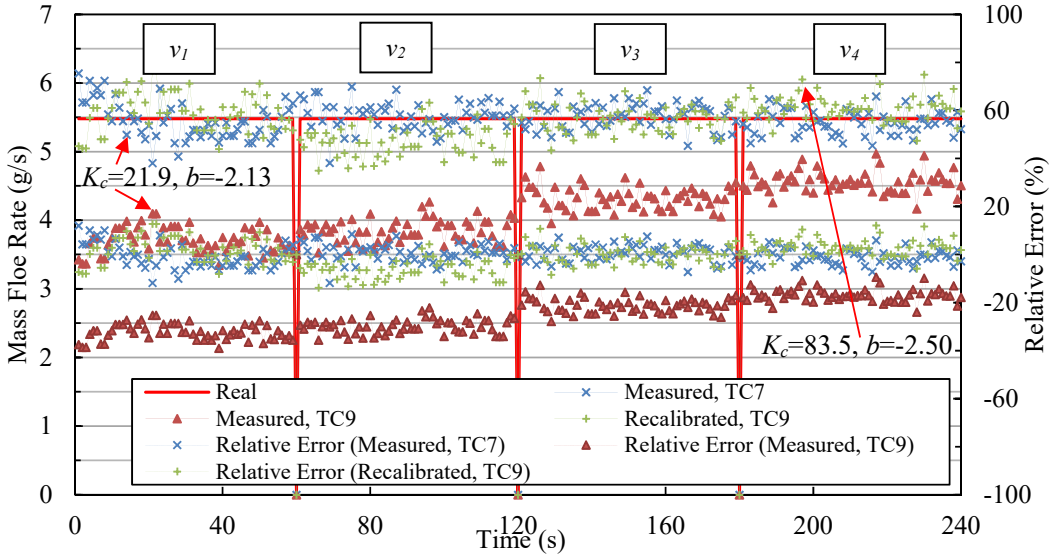

(c) Measured and recalibrated results under TC7 and TC9.

Figure 9. Measured and recalibrated results under different moisture content and particle velocity conditions.

4.3. Activated carbon results

The ambient temperature and relative humidity in the activated carbon powder tests were 23.8˚C and 40%, respectively. Figure 10 shows the raw electrostatic signals measured by both exposed and insulated electrodes with 10 mm width under TC10 and TC11, respectively, when the particle velocity was 12.5 m/s. As can be seen from Figure 10, the maximum absolute value of electrostatic amplitude is over 0.80 V under TC10, while the value is less than 0.71 V under TC11. The rms charge levels of

activated carbon powder also decrease as the moisture content increases. The mean absolute rms values from exposed and insulated electrodes under TC10 are 0.21 V and 0.09 V, and 0.18 V and 0.08 V under TC11.

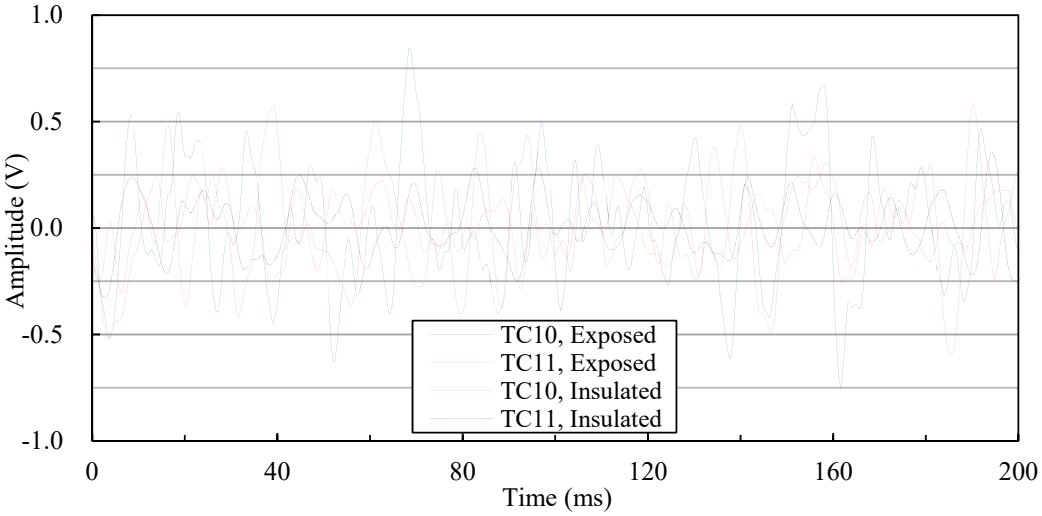

Figure 10. Electrostatic signals of activated carbon powder under different moisture content conditions.

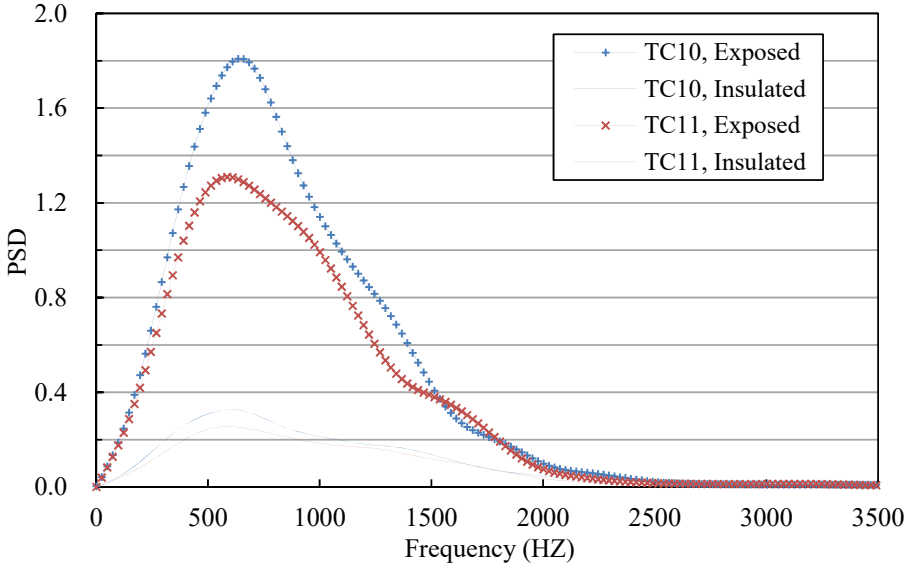

Figure 11. PSD of the electrostatic signals for activated carbon powder under different moisture content conditions.

Figure 11 shows the corresponding PSD of electrostatic signal under TC10 and TC11. The main frequencies from the signals of exposed electrode are 635 Hz and 586 Hz under TC10 and TC11, respectively, while those of the insulated electrode are 610 Hz and 586 Hz. Similar to the results obtained in the glass beads tests (Figure 6), the main frequency of electrostatic signal decreases with

the moisture content.

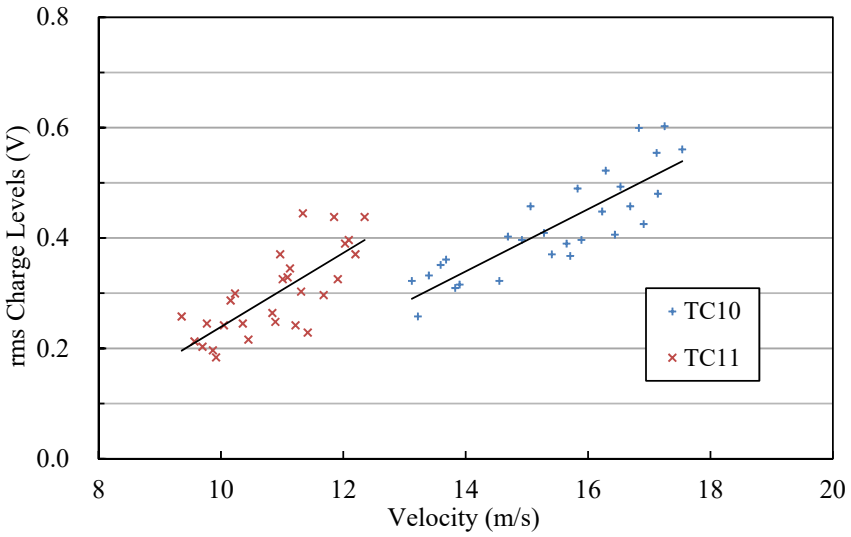

(a) rms charge levels.

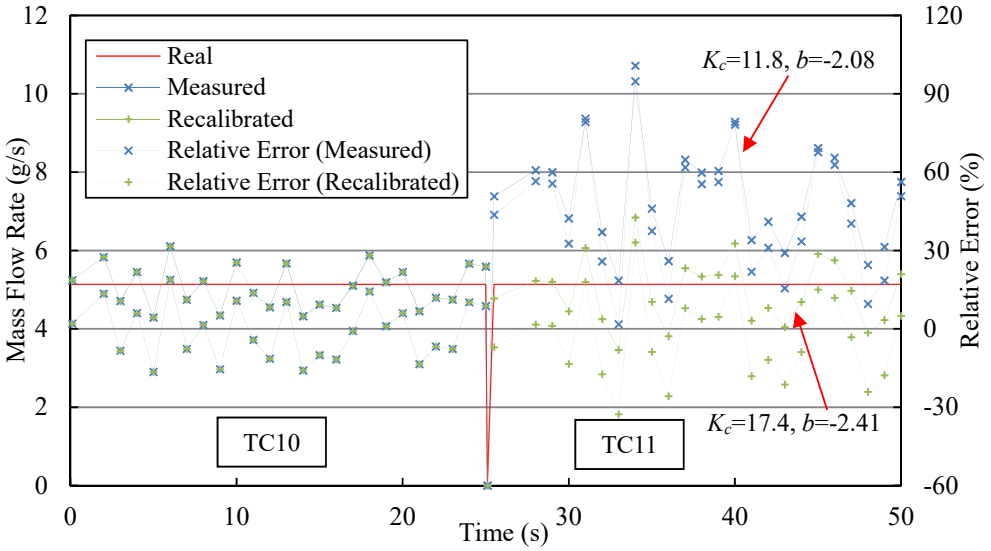

(b) Measured and recalibrated values.

Figure 12. Measured and recalibrated values of activated carbon under TC10 and TC11.

Figure 12 (a) shows the rms charge levels of the activated carbon powder under TC10 and TC11, respectively, with the increase of particle velocity. As can be seen from Figure 12(a), the measured rms charge levels become greater with the particle velocity. The coefficients K_c and b that are determined using the test data under TC10 are applied to TC11, as shown in Figure 12(b). The relative error varies within the range of ±19% when the active carbon powder has a moisture content of 3.5% and increases up to a maximum of 100% when the moisture content increases to 6.7%. Therefore,

moisture content has a more significant effect on the mass flow rate measurement of the porous activated carbon powder than the glass beads. Experimental data under TC10 and TC11 are used independently to determine K_c and b for each test condition, and the recalibrated results are shown in Figure 12 (b). Although the relative error under TC11 is still slightly greater than those under TC10, the relative errors of the measured mass flow rate under two moisture conditions are reduced to ±33% with standard deviations 0.55 and 0.85, respectively.

5. Conclusions

The rms charge levels of both nonporous glass beads and porous activated carbon powder decrease with the moisture content and, thus, result in unpredictable errors on mass flow measurement of pneumatically conveyed particles. The reduction in the rms value is greater when the particles move at a higher velocity. Furthermore, moisture content affects porous materials more on electrostatic sensing based mass flow measurement as the measurement error increases as high as 100% with moisture content, while the maximum measurement error in glass beads tests is under ±39%. The main frequency of the electrostatic signals trends to decrease with moisture content. Apart from moisture content, particle velocity plays a vital role on electrostatic sensing based mass flow measurement and the combined effect of particle velocity and moisture content is larger than either of them alone. Under different moisture conditions, a recalibration process of the coefficients K_c and b, which are used to derive particle mass flow rate, was performed and a minimum 20% reduction of measurement error has been achieved. Therefore, the electrostatic sensing based mass flow instrument is capable of providing reliable mass flow rate measurement of pneumatically conveyed particles under variable moisture content conditions when recalibration procedures are performed.

Acknowledgments

Acknowledgments are made to the Chinese Ministry of Education (B13009), Beijing Natural Science Foundation (3162031) and the Fundamental Research Funds for the Central Universities from North China Electric Power University (2016MS40) for funding this research. The authors would also like to thank Dr. Yonghui Hu, Dr. Xiaobin Huang and Miss. Shan Gu for their assistance on the electronic

circuit design, implementation of the flow test rig and signal processing.

Reference

[1] G. Klinzing, Solids flow measurements - The key to a successful operation and practice, 11th International Conference on Bulk Materials Storage, Handling and Transportation, Australia, 2013.

[2] H. Masuda, S. Matsusaka, S. Nagatani, Measurement of powder flow rate in gas–solids pipe flow based on the static electrification of particles, *Adv. Powder Technol.* 5 (1994) 241–254.

[3] Y. Zheng, Q. Liu, Review of certain key issues in indirect measurements of the mass flow rate of solids in pneumatic conveying pipelines, *Measurement* 43 (2010) 727–734.

[4] J.B. Gajewski, Electrostatic nonintrusive method for measuring the electric charge, mass flow rate, and velocity of particulates in the two–phase gas-solid pipe flows—its only or as many as 50 years of historical evolution, *IEEE Trans*. *Ind*. *Appl*. 44 (2008) 1418–1430.

[5] S.E. Law, Electrostatic induction instrumentation for tracking andcharge measurement of airborne agricultural particulates, *Trans*. *ASAE* 18 (1975) 40–45.

[6] Y. Yan, B. Byrne, S. Woodhead, J. Coulthard, Velocity measurement of pneumatically conveyed solids using electrodynamic sensors, *Meas. Sci. Technol.* 6 (1995) 515–537.

[7] C. Xu, S. Wang, G. Tang, D. Tang, B. Zhou, Sensing characteristics of electrostatic inductive sensor for flow parameters measurement of pneumatically conveyed particles, *J. Electrostat*. 65 (2007) 582–592.

[8] J. Li, C. Xu, S. Wang, Local particle mean velocity measurement using electrostatic sensor matrix in gas–solid two-phase pipe flow, *Flow Meas. Instrum.* 27 (2012) 104–112.

[9] S. Fokeer, S. Kingman, I. Lowndes, A. Rynolds, Characterisation of the cross-sectional particle concentrationdistribution in horizontal dilute flow conveying—a review, *Chem. Eng*. *Process*. 43 (2004) 677–691.

[10] X. Qian, Y. Yan, J. Shao, L. Wang, H. Zhou, C. Wang, Quantitative characterization of pulverised coal and biomass-coal blends in pneumatic conveying pipelines using electrostatic sensor arrays and data fusion techniques, *Meas. Sci. Technol.* 23 (2012) 085307.

[11] Y. Yan, Guide to the flow measurement of particulate solids in pipelines. Part 1: fundamentals and principles, *Powder Handl. Process* 13 (2001) 343–352.

[12] E. Emery, J. Oliver, T. Pugsley, J. Sharma, J. Zhou, Flowability of moistpharmaceutical powders, *Powder Technol.* 189 (2009) 409–415.

[13] S. Matsusaka, H. Maruyama, T. Matsuyama, M. Ghadiri, Triboelectric charging of powders: A review, *Chem. Eng. Sci.* 65 (2010) 5781–5807.

[14] N. Toshiyuki, S. Takeshi, M. Hiroaki, The environment humidity effect on the tribo-charge of powder, *Powder Technol.* 135 (2003) 3643–3649.

[15] C. Liang, X. Chen, P. Xu, B. Liu, C. Zhao, C. Xu, Effect of moisture content on conveying characteristics of pulverizedcoal for pressurized entrained flow gasification, *Exp*. *Therm*. *Fluid Sci.* 35 (2011) 1143–1150.

[16] D. Fleisch, A Student's Guide to Maxwell's Equations, *Cambridge UniversityPress, UK*, 2008.

[17] T. Teimour, F. Mohd, New technique to measure particle size using electrostatic sensor, *J*. *Electrostat*. 72 (2014) 120–128.

[18] S. Matsusaka, M. Ghadiriand, H. Masuda, Electrification of an elastic sphere by repeated impacts on a metal plate, *Appl. Phys.* 33 (2000) 2311–2319.

[19] J. Cross, Electrostatic: Principle, Problem and Application, AdamHilger, Bristol, 1987.

[20] T. Ken-ichiro, T. Hiroshi, K. Hajime, M. Hiroaki, Numerical simulation of tribo-electrification of particles in a gas–solids two-phase flow, *Powder Technol.* 118 (2001) 121–129.

[21] W. Zhang, C. Wang, Y. Wang, Parameter selection in cross-correlation-based velocimetry using circular electrostatic sensors, *IEEE Trans. Instrum. Meas.* 59 (2010) 1268–1275.

[22] X. Qian, X. Huang, Y. Hu, Y. Yan, Pulverized coal flow metering on a full-scale power plant using electrostatic sensor arrays, *Flow Meas. Instrum.* 40 (2014) 185–191.

[23] G. Klinzing, A. Zaltash, C. Myler, Particle velocity measurements though electrostatic field fluctuations, *Particul. Sci. Technol.* 5 (1987) 95-104.

[24] X. Qian, Y. Yan, X. Huang, Y. Hu, Measurement of the mass flow and velocity distributions of pulverized fuel in primary air pipes using electrostatic sensing techniques, *IEEE Trans. Instrum. Meas.* 66 (2017) in press.

[25] M. David, Pneumatic Conveying Design Guide, Second Ed., Elsevier Butterworth-Heinemann, Burlington, 2004.